LIMNOLOGY
and
OCEANOGRAPHY: METHODS

Limnol. Oceanogr.: Methods 12, 2014, 830–839

Considerations for the measurement of spectrophotometric pH for ocean acidification and other studies

Mike D. DeGrandpre[1], Reggie S. Spaulding[2], Jenny O. Newton[2], Emma J. Jaqueth[1], Sarah E. Hamblock[2], Andre A. Umansky[1], and Katherine E. Harris[1]*

[1]University of Montana, Department of Chemistry and Biochemistry, Missoula, MT, 59812

[2]Sunburst Sensors, LLC, Missoula, MT 59802

Abstract

Indicator-based spectrophotometric pH is commonly used for the analysis of seawater because of its high precision and long-term reproducibility. Users come from an increasingly diverse range of disciplines, primarily motivated by studies focused on the causes and effects of ocean acidification. While the analysis is readily implemented and straightforward, there are many variables that must be predetermined or measured, all of which can contribute uncertainty to the measurement. The indicator equilibrium constant and molar absorption coefficient ratios are available in the literature, but for various reasons, the conditions of analysis can be different, creating errors. Most of the parameters are temperature, salinity, and pressure dependent, posing potential additional errors. Indicator impurities and indicator perturbation of the sample pH also create uncertainties. We systematically evaluate all of the sources of error and compute how the errors propagate into CO_2 equilibrium calculations of the partial pressure of CO_2 (pCO_2) and calcium carbonate saturation states (Ω). The primary sources of uncertainty originate from wavelength and absorbance errors in low quality or poorly functioning spectrophotometers (0.007 to 0.020 pH units) and indicator impurities (0.000 to >0.040 pH units). These errors generate pCO_2 and Ω uncertainties of 11-200 μatm and 0.08-0.38, respectively, depending upon the pH value and its uncertainty.

Overview

Long-term ocean time-series have strikingly documented the decrease in ocean pH caused by anthropogenic CO_2 (Dore et al. 2009; Bates et al. 2012); however, pH is mostly used as a thermodynamic master variable in equilibrium calculations because of its importance in aqueous reactions. It is particularly useful for calculating the speciation of inorganic carbon in seawater. When measured in combination with another inorganic carbon parameter, such as total dissolved inorganic carbon (DIC), total alkalinity (A_T), or partial pressure of CO_2 (pCO_2), the concentrations of all of the remaining inorganic carbon species can be calculated. Calcium carbonate saturation state, a critical parameter for ocean acidification studies, can also be determined with this information.

Spectrophotometry using sulfonephthalein pH indicators is the preferred method for measurement of seawater pH because of its innate reproducibility compared to glass pH electrodes (Clayton and Byrne 1993). Spectrophotometric pH measurements have been made on oceanographic cruises for many years (e.g., Byrne and Breland 1989; Clayton et al. 1995; Ohline et al. 2007), and more recently on moorings (Seidel et al. 2008; Emerson et al. 2011; Gray et al. 2011, 2012; Harris et al. 2013). These measurements are sufficiently accurate for inorganic carbon calculations (Clayton et al. 1995; Byrne et al. 1999; Gray et al. 2011), and their long-term reproducibility has made it possible to calculate anthropogenic CO_2 accumulation in the oceans (Byrne et al. 2010). Researchers who study ocean acidification effects on marine organisms in laboratory or mesocosm incubations also commonly measure spectrophotometric pH while controlling another parameter, such as pCO_2 or A_T (e.g., Fangue et al. 2010; McGraw et al. 2010).

Spectrophotometric pH is popular because it is the most straightforward analysis compared to the other commonly measured CO_2 parameters. You can readily perform these mea-

*Corresponding author: E-mail: michael.degrandpre@umontana.edu

Acknowledgments

We thank Cory Beatty (University of Montana) and Jim Beck (Sunburst Sensors) for general technical assistance and Mark Patsavas (University of South Florida) for help with the indicator purification. Robert Byrne (University of South Florida) provided valuable comments in his review. Support for this work came from the U.S. National Science Foundation (Ocean Sciences 1051757, 1051550, 0628569 and Arctic Sciences 1107346).

DOI 10.4319/lom.2014.12.830

surements if your lab is equipped with a spectrophotometer; whereas, the methods for pCO_2, DIC, and A_T require complex, specialized equipment. The simplicity of spectrophotometric pH instrumentation, however, belies the complexity of the measurement. There are numerous subtleties that must be understood to obtain the best data. Many of these methodological fine points are scattered throughout various publications or have not yet been rigorously evaluated. Moreover, many present day spectrophotometric pH users do not follow the conventional shipboard technique outlined in the standard operating procedure (SOP) (Dickson et al. 2007). These users may have other constraints, such as sample size, lack of a research-grade spectrophotometer, or no temperature control, where other sources of variability can become important. Custom-built instruments may also have optical parameters that are not within the specifications of the SOP (e.g., Seidel et al. 2008; Rérolle et al. 2013).

Here, we provide a comprehensive evaluation of spectrophotometric pH parameters using experimental data, theoretical calculations, and literature sources. These parameters include temperature (T), salinity (S), pressure (P), wavelength accuracy and bandpass, absorbance accuracy and precision, indicator purity, and indicator pH perturbations (Fig. 1). We do not include a discussion of errors that may be generated due to sampling or sample storage. Errors are put into context by showing to what extent they affect the uncertainty of calculated pCO_2 and aragonite saturation state.

Theory

The spectrophotometric pH method uses the equilibrium reaction of a diprotic sulfonephthalein pH indicator

$$HL^- \rightleftarrows H^+ + L^{2-} \quad (1)$$

where HL^- and L^{2-} are the protonated and deprotonated forms of the indicator. The fully protonated H_2L form is not present at seawater pH. The pH is calculated from the equilibrium expression,

$$K_a' = \frac{[H^+][L^{2-}]}{[HL^-]} \quad (2)$$

where K_a' is the second apparent dissociation constant. The K_a' and consequently pH are on the total hydrogen ion scale (pH_T), and this scale must be used in ocean CO_2 models to accurately predict other inorganic carbon species. See Friis et al. (2004) for a concise summary of pH scales and Dickson (1984) for more in-depth discussion. $[HL^-]$ and $[L^{2-}]$ are determined using absorbance measurements on a spectrophotometer and the linear relationship between absorbance and concentration (Beer's Law):

$$A_\lambda = {}_{HL}\varepsilon_\lambda b[HL^-] + {}_{L}\varepsilon_\lambda b[L^{2-}] \quad (3)$$

where A_λ is the absorbance at the analytical wavelength (λ), the ε's are the molar absorption coefficients for HL^- and L^{2-} and b is the optical pathlength. Eq. 3 includes contributions from both indicator species because the spectra of the two forms overlap. The two species' concentrations are then determined by absorbance measurements at two or more wavelengths. The analytical wavelengths are typically selected to correspond to the peak absorbances of the HL^- and L^{2-} forms although others have proposed using full spectra to improve precision (Ohline et al. 2007).

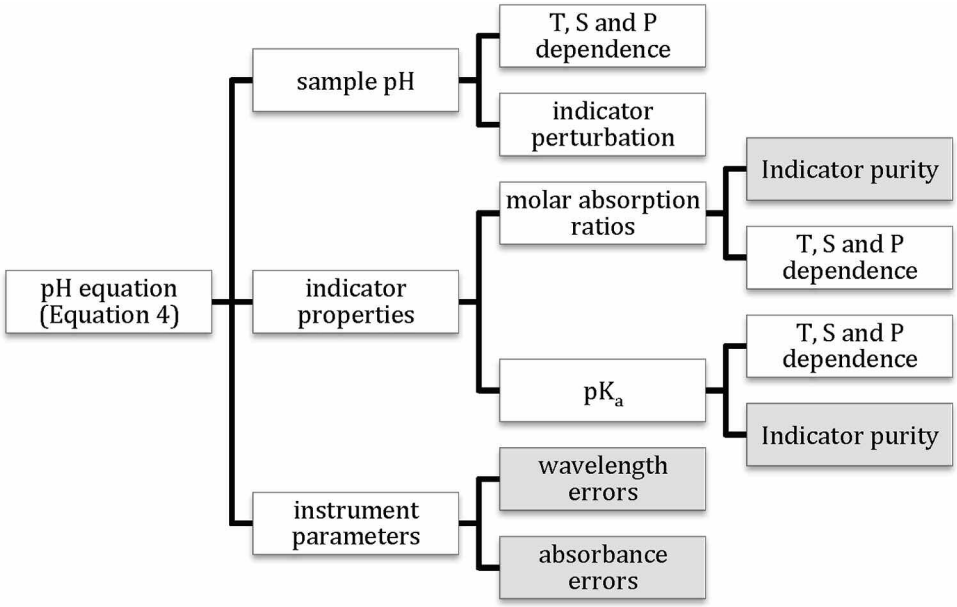

Fig. 1. Flow chart showing sources of possible errors for spectrophotometric pH measurements of seawater. Grayed boxes indicate variables that are most likely to contribute large pH errors.

A convenient form of the combined Eqs. 2 and 3, derived in Clayton and Byrne (1993), is

$$pH_T = pK_a' + \log\left(\frac{R - e_1}{e_2 - Re_3}\right) \quad (4)$$

where R is the absorbance ratio A_1/A_2 with absorbances at λ_1 and λ_2 and the e's are the ratios of the temperature-dependent molar absorption coefficients of the two species,

$$e_1 = \frac{{}^{HL}\varepsilon_{\lambda 1}}{{}^{HL}\varepsilon_{\lambda 2}} \quad e_2 = \frac{{}^{L}\varepsilon_{\lambda 1}}{{}^{HL}\varepsilon_{\lambda 2}} \quad e_3 = \frac{{}^{L}\varepsilon_{\lambda 2}}{{}^{HL}\varepsilon_{\lambda 2}} \quad (5)$$

The absorbances are determined internally by the spectrophotometer using $A_\lambda = -\log (I/I_0)$ where I_0 is the intensity transmitted through the seawater sample (i.e., blank or 100% transmittance), and I is the light intensity transmitted through the sample and indicator mixture. A modified form of Eq. 4 has been proposed by Liu et al. (2011) where e_2 is combined with pK_a'.

Numerous sulfonephthalein indicators have been used for analysis of seawater including phenol red (Robert-Baldo et al. 1985), cresol red (Byrne and Breland 1989), m-cresol purple (Clayton and Byrne 1993; Chierici et al. 1999; Friis et al. 2004), and thymol blue (Zhang and Byrne 1996; Gabriel et al. 2005). Because m-cresol purple (mCP) pK_a' is ~8.0, it is optimal for the oceanic pH range and is the indicator recommended for CO_2 system measurements (Dickson et al. 2007); therefore, this discussion focuses on the use of mCP. Recently pH errors caused by impurities in different commercial sources of mCP were quantified (Yao et al. 2007; Liu et al. 2011; Patsavas et al. 2013). Their results show the importance of using purified indicator for seawater pH measurements; therefore, we characterized the optical properties and equilibrium constant of purified mCP as part of this analysis.

Materials and procedures

pH measurements

The pH method is described in detail so that users can see potential shortcomings in their own procedures. All measurements were made with a double beam UV-VIS spectrophotometer (Varian Cary 300 Bio). The performance of the instrument is routinely checked with wavelength and absorbance standards. The Cary 300 is equipped with two water-jacketed 10 cm pathlength cell (cuvette) holders. The reference cell was filled with deionized water. For measurements below room temperature, the sample compartment was purged with N_2 to prevent condensation on the optical cell windows.

Before measurement, sample bottles were placed in a water bath set to the approximate measurement temperature. After ~20 min temperature equilibration, a 10 cm pathlength fused silica cuvette containing a stir bar was filled with sample, capped, wiped dry, and placed in the spectrophotometer. A magnetic stirring wand was mounted to the upper wall of the cell holder to mix the indicator. The external stirrer eliminated the need to remove the cell from the cell holder to manually mix the sample and indicator. The magnetic stirrer also ensured temperature homogeneity during measurement. After obtaining the blank transmittance, the cuvette cap was removed and the indicator stock solution was added using a micropipette. Sufficient indicator was added to obtain absorbances in the range of ~0.5 to 1.5 absorbance units (a.u.). Baseline absorbance was also recorded at 780 nm. All measurements were made using a 2.0 nm bandpass unless noted otherwise. The absorbance ratio R (Eq. 4) was calculated using

$$R = \frac{A_{578} - A_{780}}{A_{434} - A_{780}} \quad (6)$$

where A_{780} corrects for changes in baseline transmittance (I_0) that occur between the blank and sample measurements, e.g., due to particles or bubbles on the cell windows. Measurements were discarded if A_{780} exceeded ±0.001 a.u. After recording the absorbances, the temperature was recorded to within ±0.05°C. The cells were thoroughly cleaned weekly to remove indicator and any other organic material that adhered to the walls of the cell.

Stock mCP indicator solutions were made from the purified sodium salt of mCP (Sigma-Aldrich 211761-10G, lot 11517KC) diluted to ~1.0×10^{-3} mol kg^{-1} in 0.70 mol kg^{-1} NaCl. This solution was brought closer to seawater pH by addition of strong acid or base to minimize the pH perturbation by the indicator (see below for further discussion of the pH perturbation).

Indicator purification

Purification of the mCP sodium salt was performed using a preparative liquid chromatography system with UV detection (Teledyne-Isco Combiflash RF FPLC) and a high performance C18 column (275 g, 20-40 micron, Redi Sep RF C18aq Gold) (Patsavas et al. 2013). The mobile phase began at 5% acetonitrile:water (ACN:H_2O) and increased to 60% ACN:H_2O at 5% per minute until the purified mCP eluted. The column was then flushed with four volumes of 100% ACN. Both ACN and H_2O mobile phases included 0.05% trifluoroacetic acid (TFA, Sigma Aldrich). The TFA acts as an ion-pairing agent to minimize band broadening caused by ionized indicator. It is also volatile and is readily removed under vacuum from the concentrated eluent. The detector was set to monitor absorbance at 210 nm where both the mCP and major impurities absorb light (Liu et al. 2011). The purified mCP was collected and the solvent was evacuated under vacuum at 35°C giving a fully protonated form of mCP (formula weight = 382.43 g mol^{-1}).

Molar absorption coefficients and ratios

Molar absorption coefficient ratios (Eq. 5) for the L^{2-} and HL^- forms of purified mCP were determined at both 434 nm and 578 nm with a 2 nm bandpass. A 0.68 mol kg^{-1} NaCl solution with 0.02 mol kg^{-1} NaOH was used for the determination of the L^{2-} form (pH ~12). A sodium acetate solution with pH of ~5.0 was prepared for measurements of the HL^- form consisting of 0.018 mol kg^{-1} sodium acetate, 0.004 mol kg^{-1} HCl, and sufficient NaCl to set the ionic strength at 0.70 mol kg^{-1}

(Clayton and Byrne 1993). This pH is selected to minimize the contributions to the absorbance from the I^{2-} and H_2I forms. At pH 5.0, the I^{2-} and H_2I absorbances are negligible at 434 nm but the I^{2-} absorbance is ~2% of the HI^- absorbance at 578 nm. A 2% error in e_1, the ratio that uses the ${}_{HI}\varepsilon_{578}$, does not significantly alter the pH, as discussed below. This procedure is simplified relative to those described in Liu et al. (2011) and Clayton and Byrne (1993) who use a lower pH and iteratively determine the ε's. The absorbances were recorded for the low and high pH solutions from 0 to 40°C using the same 10 cm pathlength cell configuration described above.

pK_a' determination

We determined the pK_a' of our purified mCP by measuring the absorbances (R, Eq. 4) of mCP in tris synthetic seawater buffer (DelValls and Dickson 1998). The temperature dependence was quantified by tris measurements over the temperature range 1 to 40°C using the temperature dependent e's determined as described above and the tris pH temperature dependence (DelValls and Dickson 1998).

Equilibrium calculations

All inorganic carbon calculations were made using the program CO2SYS (Pierrot et al. 2006) with the carbonic acid dissociation constants calculated by Mehrbach et al. (1973) and refit by Dickson and Millero (1987). Nutrient concentrations were set equal to zero for these computations.

Assessment

Overview

Unlike most instrumental chemical methods, the spectrophotometric pH method has no instrument-dependent calibration factors per se; however, there are 13 variables that must be predetermined or measured for input into Eq. 4. Systematic and random pH errors can arise from these variables. We separate the parameters into those relating to the sample pH, indicator properties, and instrument parameters as shown in Fig. 1. We evaluate the uncertainty due to each variable starting with those at the top of the flow chart.

Sample pH

T, S, and P dependence

Seawater pH is dependent upon the T, S, and P of the sample when it is analyzed. Seawater pH is very temperature dependent (Gieskes 1969). The temperature sensitivity for three different marine waters ranges from –0.015 to –0.016 pH units $°C^{-1}$ (Table 1). Seawater pH decreases at higher temperatures because increased dissociation of CO_2 species leads to more H^+ in solution. Errors can be generated if the measurement temperature is inaccurate. For example, if the sample is set to be 25.0°C but cools to 24.0°C before the measurement is made, the sample pH will increase by 0.015. An error is then introduced when this pH is used in a CO_2 equilibrium model (e.g., CO2SYS) with the incorrect temperature, i.e., 25.0°C. The measured pH will not, however, be high by this amount because of other offsetting temperature-dependent errors, as described below.

Table 1. Inorganic carbon and physical properties for different surface ocean waters (P = 0 bar).

Parameter	HOT*	BATS*	Coastal*
DIC (μmol kg^{-1})	1996	2077	2014
A_T (μmol kg^{-1})	2300	2390	2180
T (°C)	25	23	11
S	35.0	36.6	32.0
pCO_2 (μatm)	390	390	390
pH	8.052	8.063	8.041
$\Omega_{aragonite}$	3.427	3.463	1.883
dpH $°C^{-1}$	–0.015	–0.015	–0.016
dpH bar^{-1}	-3.4×10^{-5}	-3.4×10^{-5}	-3.7×10^{-5}

HOT = Hawaii Ocean Time-Series (Dore et al. 2009)
BATS = Bermuda Atlantic Time-Series (Bates et al. 2012)
Coastal = Eastern Pacific waters (Harris et al. 2013)

Unlike temperature, salinity is unlikely to vary significantly during a pH analysis. Sample salinity must be known, however, because of the mCP pK_a' dependence on salinity, as described below, and also to obtain accurate equilibrium calculations using pH data. Seawater pH pressure dependence is only significant for in situ measurements at depths greater than 100 m (Table 1). Changes in lab barometric pressure are too small to have a significant effect.

Indicator perturbation

Addition of indicator, itself an acid-base species, can alter the sample pH. The modeling study by Chierici et al. (1999) estimated that the perturbation is < ±0.001 when using a 10 cm pathlength cell if the indicator solution is within ±0.3 pH units of the sample pH, e.g., in the range of 7.8-8.3 for typical sea surface pH. The perturbation error scales proportionally to pathlength because higher indicator concentrations are required to achieve a comparable absorbance in short (1 or 5 cm) pathlength cells. Although not recommended for benchtop measurements, short pathlengths are sometimes used for small volume samples (Fangue et al. 2010) or in situ analyzers (Seidel et al. 2008). Regardless of the cell used, the pH of the indicator stock solution should be adjusted by addition of HCl or NaOH to within the ranges described by Chierici et al. (1999) to minimize the pH perturbation. Alternatively, the pH perturbation can be directly determined by sequential addition of indicator to the sample and extrapolation to zero indicator concentration (Martz et al. 2003; Seidel et al. 2008). If these procedures are not followed, pH errors can be > ±0.01 pH units for 1 cm pathlength cells.

Indicator properties

Indicator molar absorption coefficient ratios

For our purified mCP the e's and their temperature-dependence in 0.7 M NaCl are

$$e_1 = 0.0049 \quad \text{(no T dependence)} \tag{7}$$

Table 2. pH errors due to absorbance precision and accuracy using mCP (see text for more details)

Example pH	absorbance ratio (R)	–0.01 a.u. accuracy ±0.001 a.u. precision	(true pH – calculated pH)
8.562	4.108	±0.0035	–0.0220
8.398	3.436	±0.0031	–0.0180
8.245	2.873	±0.0022	–0.0140
8.091	2.404	±0.0021	–0.0110
7.799	1.683	±0.0019	–0.0051
7.653	1.415	±0.0018	–0.0035

$$e_2 = -2.0168 \times 10^{-3}T + 2.2941 \quad (r^2 = 1.0000) \quad (8)$$

$$e_3 = 5.2620 \times 10^{-4}T + 0.11091 \quad (r^2 = 0.9989) \quad (9)$$

where T is in °C. These equations apply to measurements with purified mCP in high ionic strength solutions (the e's have a weak salinity dependence, see below) over the range of 0-40°C at 578 and 434 nm with a 2.0 nm bandpass. The e_2 from Eq. 8 at 24.8°C is 2.244 compared with 2.229 for purified mCP from R. Byrne (pers. comm.). The impure and purified indicators have the same temperature dependence within the uncertainty of the slope (not shown). Based on this, we assume that the T, S, and P dependence of the e's are very similar for any commercial or purified mCP.

It is important to note that e_1 does not contribute significantly to pH uncertainty because it is small relative to the absorbance ratio (R) (Table 2, Eq. 5). Setting e_1 to zero leads to pH errors no larger than 0.002 for pHs greater than 7.8, and the error is < 0.001 at typical surface seawater pH. The other e's have a weak temperature dependence: –0.15%°C^{-1} for e_2 and + 0.10%°C^{-1} for e_3 (Eqs. 8 and 9). Significant errors result, however, if values at 25°C are used for e_2 and e_3 and the sample is measured at the in situ temperature, e.g., 10°C. The more likely scenario is that the temperature at the time of measurement is inaccurate. For example, if the sample temperature is recorded to be 25°C but cools to 24°C before the measurement due to poor temperature control, a pH error of ~ +0.0008 is incurred due to incorrect e's.

The sulfonephthalein indicator e's have a weak salinity dependence (Gabriel et al. 2005; Liu et al. 2011), reflecting that molecular spectra typically are not strongly dependent on solution composition. Liu et al. (2011) estimated pH errors less than 0.0015 over the salinity range of 20 to 40. Our measurements of dilute tris (S ~25) found errors < 0.0025 when using e's with no salinity dependence (not shown). The salinity dependence should be considered and further evaluated for salinities outside the range of 20 to 40.

Ambient pressure is another environmental variable that could affect the indicator absorption characteristics. Soli et al. (2013) determined the pressure dependence of the e's for mCP. Based on their results, the e's of sulfonephthalein indicators have a very weak pressure dependence that would not affect measurements at sea level. However, for in situ measurements > 1000 m depth, the pressure dependence needs to be considered.

Indicator pK_a'

The pK_a' is also T, S, and P dependent and its accuracy also depends upon indicator impurities. As noted in Eq. 4, pK_a' errors add an equal error to the calculated pH. The pK_a' equation for our purified mCP determined over the range 0°-40°C and S = 35 is

$$pK_a' = -241.46 + 7085.7/T + 43.833\ln(T) - 0.080641T \quad (10)$$

where T is temperature in Kelvin. The residual to the fit is ±0.0009. The pK_a' is 8.0045 at 25°C and S = 35. We compared our pK_a' with Liu et al. (2011) by converting their $p(K_a' e_2)$ to pK_a' using our e_2 (Eq. 8). The mean difference is 0.0052 ±0.0008 over the typical pH range (7.6-8.3) (S = 35) (Fig. 2). These results, using a different method for determining the e's and an independently purified batch of mCP, are an important independent validation of the equation in Liu et al. (2011). The offset between the two values (Fig. 2) is likely due to small differences in the tris pH and errors from our simplified

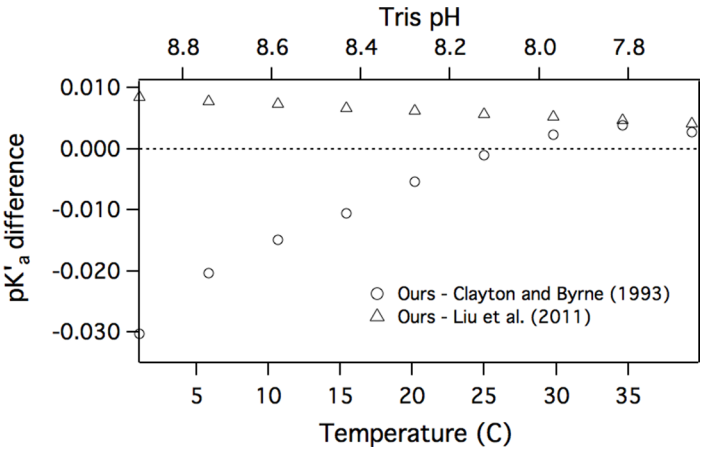

Fig. 2. Purified meta-cresol purple pK_a' comparison with Liu et al. (2011) and the pK_a' reported in Clayton and Byrne (1993) for impure mCP. Our pK_a' was determined using tris synthetic seawater buffer at different temperatures (bottom axis) (S = 35). The pH of tris for these samples is shown on the top axis.

method for determining the e's, which is only a single point absorbance measurement. We recommend use of the Liu et al. (2011) equation for pH analyses with purified mCP except as noted below.

The mean pK_a' temperature dependence is $-0.0140°C^{-1}$ and varies by ~$0.001°C^{-1}$ over the seawater temperature range. This potential error, however, is nearly canceled by the error in sample pH for small temperature errors (Byrne and Breland 1989; Dickson et al. 2007). For example, if the temperature of the sample is assumed to be 25°C but is 24°C, sample pH will be high by ~0.015 but the pK_a' will be calculated at 25°C and will be ~0.014 low; therefore, the calculated pH will be within 0.001 of the true pH at 25°C. These same arguments do not apply to synthetic tris seawater because it is ~2 times more sensitive to temperature changes than seawater. For measurements in tris, the scenario described above would result in a +0.015 pH error.

The pK_a' is not very sensitive to errors in S and P. The Liu et al. (2011) equation indicates that salinity errors of ±1 result in a pH error of ~ ±0.002 at room temperature and ~ ±0.001 at 1°C. The pressure dependence of the mCP pK_a' is approximately 0.00019 bar^{-1} (Soli et al. 2013); therefore only pressures > 10 bar (~100 m depth) have a significant effect (~0.002 pH units).

Although not fully appreciated until recently (Yao et al. 2007; Liu et al. 2011), indicator impurities create significant systematic errors that depend upon the sample pH and indicator vendor (Fig. 2a in Liu et al. 2011). Errors due to indicator impurity became embedded in the pK_a' in earlier pK_a' determinations. In Clayton and Byrne (1993), the mCP pK_a' was determined in tris seawater buffer at 25°C using Eq. 4, but because the dye impurity affects the e's, the log term in Eq. 4 was not accurate embedding an error in the pK_a'. Comparison of the purified mCP pK_a' from Eq. 10 with that reported in Clayton and Byrne (1993) for impure mCP shows the effect of indicator impurities on the pK_a' accuracy (Fig. 2). Some of the impurities absorb light at the same wavelengths as the HL^- form of the indicator based on chromatographic separation data (Yao et al. 2007; Liu et al. 2011). The error increases with increasing pH because the HI^- A_{434} decreases at higher pH but the absorbance of the impurities remains constant causing R to be smaller than it should be (Yao et al. 2007). Consequently, the estimated pK_a' is systematically high (solving Eq. 4 for pK_a' where pH is the pH of tris). These errors can be as large as 0.02 at pH of 8.2 for some commercial mCP sources.

Instrument parameters

Wavelength and bandpass related errors

Spectrophotometric pH analyses implicitly assume that the analytical wavelengths and bandpass are identical to those used to determine the e's (Eq. 5). It is possible, however, to perform analyses, either knowingly or unknowingly, with incorrect or inaccurate settings. We examined the sensitivity to these parameters by performing analyses with different wavelengths and bandpasses. The absorbance ratio (R) was then used in Eq. 4 to determine the pH error.

Absorbances were recorded around the wavelengths normally used for pH analyses to examine wavelength errors. Tris buffer was used as the sample (pH = 8.059 at 25°C). Absorbance drops significantly on either side of the relatively narrow I^{2-} absorbance peak (Fig. 3). If the spectrophotometer wavelength deviates from the analytical wavelength prescribed by the e (578 nm, Eq. 5), the absorbance ratio R (A_{578}/A_{434}) will be low. A ±4 nm error leads to a pH low by ~0.005 (Fig. 4). The symmetry of the error around 578 nm reflects the symmetry of the absorbance peak. Around the 434 nm peak, absorbance decreases (R increases) at shorter wavelengths but increases (R decreases) at longer wavelengths due to the increasing absorbance of the I^{2-} form (Fig. 3). The resulting R errors lead to a positive systematic pH error at short wavelengths and a negative error at long wavelengths. If the wavelength error is the same at both analytical wavelengths (a

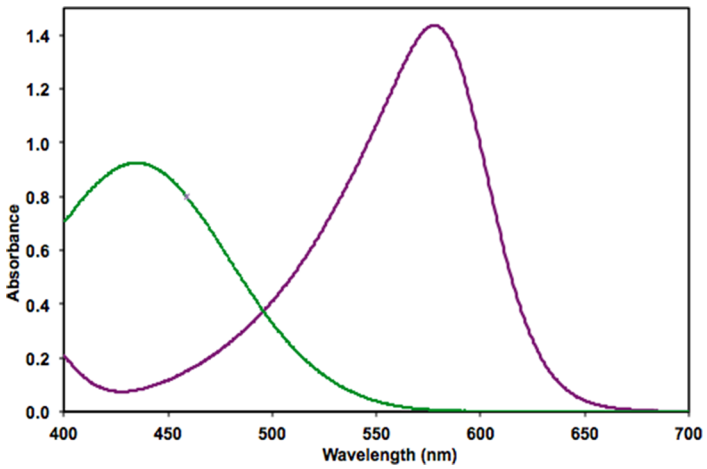

Fig. 3. Absorbance spectra of the HI^- (green, 51.4 μmol kg^{-1}) and I^{2-} (purple, 36.5 μmol kg^{-1}) forms of meta-cresol purple (mCP) (not purified). Pathlength = 1 cm.

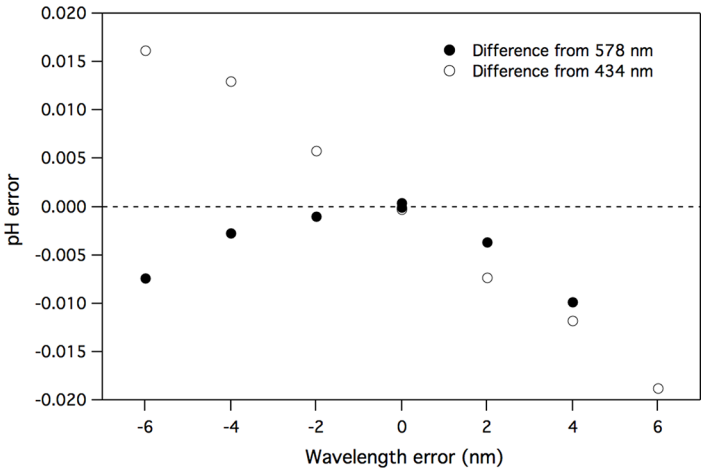

Fig. 4. pH errors (measured pH - tris pH) due to wavelength accuracy errors (tris actual pH = 8.059). See text for discussion.

more likely scenario because a faulty wavelength calibration would offset the whole spectrum), the pH error levels off at ~ +0.005 pH units at the short wavelengths but further increases at long wavelengths (–0.007 pH units at +4 nm, not shown). Results were similar for measurements at a higher pH (8.5). Wavelength errors would not typically be a concern because even low quality instruments have quoted uncertainties of at most ±2 nm but instruments can lose their wavelength calibration. It is essential to periodically check wavelength accuracy using a wavelength standard such as a holmium oxide glass filter. In custom-made systems, bandpass filter wavelengths can also vary significantly from the mCP peak wavelengths (e.g., Seidel et al. 2008).

The bandpass effects on pH accuracy were tested with the three different bandpasses available on the Cary 300 UV-VIS: 0.5, 2.0, and 4.0 nm. The pH errors using the 0.5 and 4.0 nm bandpasses relative to the 2.0 nm bandpass were +0.0002 and –0.0024 pH units, respectively (not shown). With the larger bandpass, A_{578} decreases more than the A_{434} due to the narrower peak at 578 nm resulting in a low pH relative to that measured with 2.0 nm bandpass. While these errors are small, low-quality spectrophotometers or custom-made systems may have a large minimum bandpass (e.g., 8 nm) to improve light throughput, and users of these instruments need to quantify the error using tris buffer. If the pH errors associated with these parameters are not acceptable, users will need to determine the e's or purchase a system with suitable specifications. If the former, the e's will be specific to the instrument and potentially not appropriate for other spectrophotometric systems.

Absorbance precision

Specifications for absorbance precision and accuracy vary widely between spectrophotometers. The sensitivity to these parameters was examined by varying the absorbances in Eq. 6 (A_{434}, A_{578}, A_{780}) obtained for tris samples over the pH range from 7.65 to 8.56 (Table 2). An absorbance precision of ±0.001 a.u. leads to average pH errors of ±0.0024 and the precision degrades from ±0.0018 to ±0.0035 from pH 7.65 to 8.56, respectively. The pH standard deviation is larger at high pH because A_{434} is low (<0.2 a.u.) and the relative error is larger. Absorbance precision levels, also known as photometric noise in instrument specification sheets, are typically < ±0.001 a.u. and as low as ±0.0005 a.u. for high quality spectrophotometers. The photometric noise would ideally control pH precision but other factors such as changes in transmittance due to cuvette placement, bubbles in the optical path, incomplete mixing of indicator, and temperature fluctuations can lead to larger replicate uncertainty. However, with practice, analysts should be able to achieve pH reproducibility < ±0.003 and as low as ±0.0004 (Clayton and Byrne 1993).

Absorbance accuracy

Absorbance accuracy, also known as photometric accuracy, was examined by assuming stray light (light transmitted through the sample that is outside the selected bandpass) is the source of error and also by assuming a constant error of 0.01 a.u. Stray light leads to increasing absorbance errors and nonlinearity as absorbance increases because it becomes a larger component of the transmitted signal. With a stray light level of 0.1% of the blank transmittance, a typical value for lower quality spectrophotometers, errors only become large (~0.005 pH units), at high pH when A_{578} is potentially large (>1.5). Errors are insignificant at lower pHs because, with the lower HI^- molar absorptivity coefficient (Fig. 3), A_{434} is never large enough for stray light to significantly affect the absorbance.

Absorbance inaccuracy due to other factors can be as high as 0.01 a.u. quoted by some instrument manufacturers. This error leads to large systematic pH errors when both A_{434} and A_{578} are reduced (or increased) by 0.01 a.u. (Table 2). With –0.01 a.u. absorbance errors and the R's in Table 2, the pH's are systematically high because A_{434} is decreased disproportionately relative to A_{578} making R too large. Analysts should check absorbance accuracy specifications of their instrument, routinely use absorbance standards (e.g., NIST absorbance standards), and measure tris seawater buffer to determine if the spectrophotometer accuracy is limiting pH accuracy.

Discussion, implications, and recommendations

Assuming pH sampling is done correctly, the primary sources of uncertainty in spectrophotometric pH measurements originate from low quality or poorly functioning spectrophotometers and indicator impurities. Absorbance and wavelength accuracy issues can be readily minimized by using mid to high quality spectrophotometers and routinely checking their performance. If the specifications are suitable, the equations in Liu et al. (2011) can be used with purified mCP to calculate the pH. Indicator purity errors are more problematic, especially for samples with pHs > 8.2, e.g., in coastal areas (Harris et al. 2013). Most users will not be able to purify their own indicator but some labs are now providing mCP to the broader community (R. Byrne pers. comm.).

We strongly encourage labs that routinely perform spectrophotometric pH analyses to use tris seawater buffers to verify performance. These buffers can be reproducibly prepared using the recipe in DelValls and Dickson (1998). High purity salts can be purchased and further purification is not necessary, greatly simplifying the method in DelValls and Dickson (1998). Our batches of tris have been within –0.0012 ±0.0025 pH units of the recipe value (n = 17) without purification of the salts. Moreover, tris pH can be varied over a wide range (~7.6-8.9) by varying the analysis temperature (Fig. 2), if temperature control is available. It is important to remember, however, that the tris temperature must be known to within ~0.1°C to obtain accuracy of < 0.0015 pH units.

As noted above, the e's must be accurately known to obtain the best quality measurements. Eq. 10 offers an alternative to the e-dependent Liu et al. (2011) $p(K_a' e_2)$ equation for situations where the instrument parameters are significantly differ-

ent from 434 and 578 nm and a 2.0 nm bandpass, such as in custom-designed instruments that do not use a grating spectrograph. If Eq. 10 is used, the salinity dependence can be determined from the Liu et al. (2011) equation.

The pH uncertainties above must be put in context of the error that is generated when pH is used in CO_2 equilibrium calculations. The errors in aragonite saturation state (Ω_{Ar}) and pCO_2 calculated from pH and A_T were determined by varying the pH uncertainty over a broad range while keeping the A_T constant (2300 μmol kg^{-1}). These calculations show that pH uncertainties of ~0.01 lead to relatively small errors in Ω_{Ar} and pCO_2, with larger errors at high and low pH, respectively (Fig. 5). Including an A_T uncertainty of ~0.2% (±4 μmol kg^{-1}) adds uncertainty of ~ ±0.06 to Ω_{Ar} and ~ ±6 μatm to pCO_2 to the error contours in Fig. 5. These errors might be acceptable for some applications such as mesocosm studies but not for others, such as air-sea flux (pCO_2) estimates. Errors in the dissociation constants can also significantly increase the uncertainty of calculated parameters (e.g., Hoppe et al. 2012) but are not considered here.

Spectrophotometric measurements of seawater pH offer distinct advantages in terms of analytical simplicity and can provide reproducible and precise results if the precautions outlined here and elsewhere (Dickson et al. 2007) are followed. Similar considerations apply to the spectrophotometric measurement of freshwater pH (Yao and Byrne 2001) although additional precautions to minimize the indicator pH perturbation may be required (Yuan and DeGrandpre 2008).

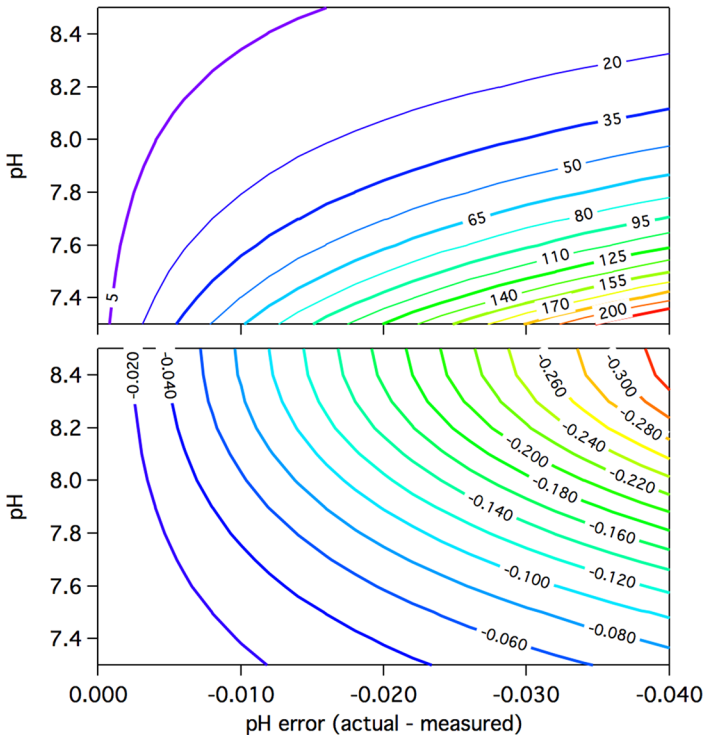

Fig. 5. Theoretical errors in pCO_2 (μatm) (top) and aragonite saturation state (bottom) caused by pH errors over the seawater pH range. These calculations were made using CO2SYS with A_T = 2300 μmol kg^{-1} at T = 25°C and S = 35. Including an A_T uncertainty of ~0.2% (~4 μmol kg^{-1}) adds uncertainty of ~ ±0.06 to Ω_{Ar} and ~ ±6 μatm to pCO_2. This analysis does not include uncertainty in the equilibrium constants.

References

Bates, N. R., M. H. P. Best, K. Neely, R. Garley, A. G. Dickson, and R. J. Johnson. 2012. Detecting anthropogenic carbon dioxide uptake and ocean acidification in the North Atlantic Ocean. Biogeosciences 9:2059-2522.

Byrne, R. H., and J. A. Breland. 1989. High precision multiwavelength pH determinations in seawater using cresol red. Deep-Sea Res. I 36:803-810 [doi:10.1016/0198-0149(89)90152-0].

———, S. McElligott, R. A. Feely, and F. J. Millero. 1999. The role of pH_T measurements in marine CO_2-system characterization. Deep-Sea Res. 46:1985-1997 [doi:10.1016/S0967-0637(99)00031-X].

———, S. Mecking, R. A. Feely, and X. Liu. 2010. Direct observations of basin-wide acidification of the North Pacific Ocean. Geophys. Res. Lett. 37:L02601 [doi:10.1029/2009GL040999].

Chierici, M., A. Fransson, and L. G. Anderson. 1999. Influence of m-cresol purple indicator additions on the pH of seawater samples: correction factors evaluated from a chemical speciation model. Mar. Chem. 65:281-290 [doi:10.1016/S0304-4203(99)00020-1].

Clayton, T. D., and R. H. Byrne. 1993. Spectrophotometric seawater pH measurements: total hydrogen ion concentration scale calibration of m-cresol purple and at-sea results. Deep-Sea Res. I 40:2115-2129 [doi:10.1016/0967-0637(93)90048-8].

———, and others. 1995. The role of pH measurements in modern oceanic CO_2-system characterizations: precision and thermodynamic consistency. Deep-Sea Res. II 42:411-429 [doi:10.1016/0967-0645(95)00028-O].

DelValls, T. A., and A. G. Dickson. 1998. The pH of buffers based on 2-amino-2-hydroxymethyl-1,3-propanediol (tris) in synthetic sea water. Deep-Sea Res. I 45:1541-1554 [doi:10.1016/S0967-0637(98)00019-3].

Dickson, A. G. 1984. pH scales and proton-transfer reactions in saline media such as sea water. Geochim. Cosmochim. Acta 48:2299-2308 [doi:10.1016/0016-7037(84)90225-4].

———, and F. J. Millero. 1987. A comparison of the equilibrium-constants for the dissociation of carbonic-acid in seawater media. Deep-Sea Res. I 34:1733-1743 [doi:10.1016/0198-0149(87)90021-5].

———, C. L. Sabine, and J. R. Christian (Eds.). 2007. Guide to best practices for ocean CO_2 measurements. PICES Special Publication 3.

Dore, J. E., R. Lukas, D. W. Sadler, M. J. Church, and D. M. Karl. 2009. Physical and biogeochemical modulation of ocean acidification in the central North Pacific. Proc. Nat. Acad. Sci. 106:12235-12240 [doi:10.1073/pnas.0906044106].

Emerson, S., C. L. Sabine, M. Cronin, S. E. Cullison and M. D. DeGrandpre. 2011. Production rates of $CaCO_3$ and organic carbon in ocean surface waters from in situ measurements of pCO_2 and pH. Global Biogeochem. Cycles. 25:GB3008 [doi:10.1029/2010GB003924].

Fangue, N. A., M. J. O'Donnell, M. A. Sewell, P. G. Matson, A. C. MacPherson, and G. E. Hofmann. 2010. A laboratory-based, experimental system for the study of ocean acidification effects on marine invertebrate larvae. Limnol. Oceanog. Methods 8:441-452 [doi:10.4319/lom.2010.8.441].

Friis, K., A. Körtzinger, and D. W. R. Wallace. 2004. Spectrophotometric pH measurement in the ocean: Requirements, design, and testing of an autonomous charge-coupled device detector system. Limnol. Oceanogr. Methods 2:126-136 [doi:10.4319/lom.2004.2.126].

Gabriel, M. D., J. M. Forja, J. A. Rubio, and A. Gomez-Parra. 2005. Temperature and salinity dependence of molar absorptivities of thymol blue: application to the spectrophotometric determination of pH in estuarine waters. Cienc. Mar. 31:309-318.

Gieskes, J. M. 1969. Effect of temperature on the pH of seawater. Limnol. Oceanogr. 14:679-685 [doi:10.4319/lo.1969.14.5.0679].

Gray, S. E., M. D. DeGrandpre, T. M. Moore, T. R. Martz, G. E. Friederich, and K. S. Johnson. 2011. Applications of in situ pH measurements for inorganic carbon calculations. Mar. Chem. 125:82-90 [doi:10.1016/j.marchem.2011.02.005].

———, M. D. DeGrandpre, C. Langdon, and J. E. Corredor. 2012. Short-term and seasonal pH, pCO_2 and saturation state variability in a coral-reef ecosystem. Global Biogeochem. Cycles 26:GB3012 [doi:10.1029/2011GB004114].

Harris, K. E., M. D. DeGrandpre, and B. Hales. 2013. Aragonite saturation state dynamics in a coastal upwelling zone. Geophys. Res. Lett. 40:1-6 [doi:10.1002/grl.50460].

Hoppe, C. J. M., G. Langer, S. D. Rokitta, D. A. Wolf-Gladrow, and B. Rost. 2012. Implications of observed inconsistencies in carbonate chemistry measurements for ocean acidification studies. Biogeosciences 9:2401-2405 [doi:10.5194/bg-9-2401-2012].

Liu, X. W., M. C. Patsavas, and R. H. Byrne. 2011. Purification and characterization of meta-cresol purple for spectrophotometric seawater pH measurements. Environ. Sci. Technol. 45:4862-4868 [doi:10.1021/es200665d].

Martz, T. R., J. J. Carr, C. R. French, and M. D. DeGrandpre. 2003. A submersible autonomous sensor for spectrophotometric pH measurements of natural waters. Anal. Chem. 75:1844-1850 [doi:10.1021/ac020568l].

Mehrbach, C., C. H. Culberson, J. E. Hawley, and R. M. Pythowicz. 1973. Measurement of the apparent dissolution dissociation constants of carbonic acid in seawater at atmospheric pressure. Limnol. Oceanogr. 18:897-907 [doi:10.4319/lo.1973.18.6.0897].

McGraw, C. M., and others. 2010. An automated pH-controlled culture system for laboratory-based ocean acidification experiments. Limnol. Oceanogr. Methods 8:686-694 [doi:10.4319/lom.2010.8.686].

Ohline, S. M., M. R. Reida, S. L. G. Husheer, K. I. Currie, and K. A. Hunter. 2007. Spectrophotometric determination of pH in seawater off Taiaroa Head, Otago, New Zealand: full-spectrum modelling and prediction of pCO_2 levels. Mar. Chem. 107:143-155 [doi:10.1016/j.marchem.2007.06.018].

Patsavas, M. C., R. H. Byrne, and X. Liu. 2013. Purification of meta-cresol purple and cresol red by flash chromatography: Procedures for ensuring accurate spectrophotometric seawater pH measurements. Mar. Chem. 150:19-24 [doi:10.1016/j.marchem.2013.01.004].

Pierrot, D., E. Lewis, and D. W. R. Wallace. 2006. MS Excel program developed for CO_2 system calculations, ORNL/CDIAC-105a. U.S. Dep. of Energy [doi:10.3334/CDIAC/otg.CO2SYS_XLS_CDIAC105a].

Rérolle, V. M. C., C. F. A. Floquet, A. J. K. Harris, M. D. Mowlem, R. G. J. Bellerby, and E. R. Achterberg. 2013. Development of a colorimetric microfluidic pH sensor for autonomous seawater measurements. Anal. Chim. Acta 786:124-131 [doi:10.1016/j.aca.2013.05.008].

Robert-Baldo, G., M. J. Morris, and R. H. Byrne. 1985. Spectrophotometric determination of seawater pH using phenol red. Anal. Chem. 57:2564-2567 [doi:10.1021/ac00290a030].

Seidel, M. P., M. D. DeGrandpre, and A. G. Dickson. 2008. A sensor for in situ indicator-based measurements of seawater pH. Mar. Chem. 109:18-28 [doi:10.1016/j.marchem.2007.11.013].

Soli, A. L., B. J. Pav, and R. H. Byrne. 2013. The effect of pressure on meta-Cresol Purple protonation and absorbance characteristics for spectrophotometric pH measurements in seawater. Mar. Chem. 157:162-169 [doi:10.1016/j.marchem.2013.09.003].

Yao, W., and R. H. Byrne. 2001. Spectrophotometric determination of freshwater pH using bromocresol purple and phenol red. Environ. Sci. Technol. 35:1197-1201 [doi:10.1021/es001573e].

———, X. Liu, and R. H. Byrne. 2007. Impurities in indicators used for spectrophotometric seawater pH measurements: assessment and remedies. Mar. Chem. 107:167-172 [doi:10.1016/j.marchem.2007.06.012].

Yuan, S., and M. D. DeGrandpre. 2008. Evaluation of indicator-based pH measurements for freshwater over a wide range of buffer intensities. Environ. Sci. Technol. 42:6092–6099 [doi:10.1021/es800829x].

Zhang, H., and R. H. Byrne. 1996. Spectrophotometric pH measurements of surface seawater at in situ conditions: absorbance and protonation behavior of thymol blue. Mar. Chem. 52:17-25 [doi:10.1016/0304-4203(95)00076-3].

Submitted 15 September 2014
Revised 3 November 2014
Accepted 3 November 2014